Evolutionary branching points in multi-dimensional trait spaces

Hiroshi C. Ito [a] and Akira Sasaki [a,b]

[a] Research Center for Integrative Evolutionary Science, The Graduate University for Advanced Studies, SOKENDAI, Hayama, Kanagawa 240-0193, Japan

[b] Evolution and Ecology Program, International Institute for Applied Systems Analysis, A-2361 Laxenburg, Austria

Abstract

Ecological interaction can induce evolutionary diversification of a biological population into distinct multiple populations. Such a process is called evolutionary branching in adaptive dynamics theory. In one-dimensional trait spaces, the existence of an evolutionary branching point ensures evolutionary branching of an asexual monomorphic population in its neighborhood under rare and small mutations. An evolutionary branching point is a convergence stable point (i.e., a point attractor for a monomorphic population through directional selection) that is not an ESS (evolutionarily stable strategy). For analysis of arbitrary higher-dimensional trait spaces with respect to evolutionary branching induced by convergence stable non-ESSes, this study develops two kinds of criteria. The two criteria, referred to as branching possibility and branching inevitability, are based respectively on the canonical equation of adaptive dynamics theory and on the local Lyapunov function. The branching possibility ensures the existence of evolutionary paths achieving evolutionary branching. The branching inevitability ensures steady progress of evolutionary branching through repeated invasions by arbitrary mutants having positive invasion fitnesses, even when the timescale separation between population dynamics and evolutionary dynamics is incomplete.

1 Introduction

Ecological interaction can induce evolutionary diversifications of biological populations, including speciation (Dieckmann et al. 2004) and adaptive radiation (Schluter 2000). In adaptive dynamics theory, evolutionary diversification of a biological population into distinct multiple populations through ecological interaction is called evolutionary branching (Metz et al. 1996; Geritz et al. 1997). For a population evolving in a one-dimensional trait space, the likelihood of its evolutionary branching is well characterized by whether the space has evolutionary branching points (Metz et al. 1996; Geritz et al. 1997). An evolutionary branching point is a convergence stable point, i.e., a point attractor for a monomorphic population through directional selection (Eshel 1983), that is not evolutionarily stable, i.e., the population still can be invaded by some mutants even when it has reached the point (Maynard Smith and Price 1973).

In the higher-dimensional trait spaces, evolutionary dynamics is potentially more complex (Doebeli and Ispolatov 2010). In particular, multi-dimensional trait spaces have three classes of

convergence stability: (normal) convergence stability, strong convergence stability, and absolute convergence stability (Leimar 2009), where convergence stable points include strongly convergence stable points, and strongly convergence stable points include absolute convergence stable points.

So far, strongly convergence stable non-ESSes have been treated as candidates for evolutionary branching points (Vukics et al. 2003; Ackermann and Doebeli 2004; Ito and Shimada 2007; Ito and Dieckmann 2012, 2014; Geritz et al. 2016; Ito and Sasaki 2016, 2020). Geritz et al. (2016) derived a set of conditions ensuring that the initial divergent evolution of slightly differentiated morphs in trait spaces of arbitrary dimensions result in dimorphic divergence without collapse into a single morph, by describing their evolution with coupled Lande's equations (Lande 1979). While these conditions are satisfied by strongly convergence stable non-ESSes in two-dimensional trait spaces, the higher-dimensional cases remain to be analyzed further (Geritz et al. 2016).

In the present study, we develop analytically tractable two criteria for qualitatively evaluating the likelihood of evolutionary branching. The two criteria, referred to as the branching possibility and branching inevitability, are based respectively on the canonical equation of adaptive dynamics theory (Dieckmann and Law 1996) and on the local Lyapunov function. For trait spaces of arbitrary dimensions, we derive that the branching possibility is warranted not only for strongly convergence stable non-ESSes but also for convergence stable non-ESSes that do not have strong convergence stability but do satisfy the conditions for locally stable dimorphic divergence. We also show that all absolutely convergence stable non-ESSes have the branching inevitability; there exist local Lyapunov functions ensuring steady progress of evolutionary branching even without timescale separation between population dynamics and evolutionary dynamics, provided that the population dynamics is deterministic.

The reminder of this paper is structured as follows. Section 2 describes the basic framework of adaptive dynamics theory for multi-dimensional trait spaces. Section 3 describes the branching possibility conditions and branching inevitability conditions and then show whether convergence stable non-ESSes of each convergence class may have either or both branching possibility and inevitability. Section 4 shows a simple application example for the developed branching point conditions. Section 5 discusses the present results in connection with relevant studies.

2 Framework of adaptive dynamics theory for multi-dimensional trait spaces

In this section, we explain the basic assumptions and concepts in adaptive dynamics theory for multi-dimensional trait spaces.

2.1 Basic assumptions and evolutionarily singular points

We consider a trait space $\mathbf{s} = (x_1, \dots, x_L)^{\mathrm{T}}$ of an arbitrary dimension denoted by L (≥ 2) and suppose M coexisting phenotypes $\mathbf{s}_1, \dots, \mathbf{s}_M$. We write the dynamics of their population sizes $n_1, \dots, n_M$ as

$$\frac{dn_i}{dt} = n_i F(\boldsymbol{s}_i; (\boldsymbol{s}_1, \dots, \boldsymbol{s}_M), (n_1, \dots, n_M)), \tag{1}$$

where $F(\mathbf{s}_i; (\mathbf{s}_1, \dots, \mathbf{s}_M), (n_1, \dots, n_M))$ describes the fitness of phenotype $\mathbf{s}_i = \left(x_{i,1}, \dots, x_{i,L}\right)^{\mathrm{T}}$.

We assume that this fitness function satisfies the applicability conditions of adaptive dynamics theory (Ito et al. 2020). We also assume sufficiently low mutation rates and small mutational step sizes such that the population dynamics is almost at equilibrium whenever a mutant emerges, in which case the evolutionary dynamics can be described as a sequential transitions of resident phenotypes formed by repeated mutant invasions, called a trait substitution sequence (Metz et al. 1996). When there exists only a monomorphic population with its resident phenotype $\mathbf{s} = (x_1, \dots, x_L)^{\mathrm{T}}$ at its equilibrium population size $\hat{n}$, a mutant $\mathbf{s}' = (x_1', \dots, x_L')^{\mathrm{T}}$ can invade if it has a positive invasion fitness, given by its initial par-capita growth rate:

$$f(\mathbf{s}'; \mathbf{s}) = \lim_{n' \to 0} F(\mathbf{s}'; (\mathbf{s}', \mathbf{s}), (n', \hat{n})) \tag{2}$$

with n' describing the mutant's population size. As long as the fitness gradient at $\mathbf{s}$, given by

$$\mathbf{g}(\mathbf{s}) = \begin{pmatrix} g_1(\mathbf{s}) \\ \vdots \\ g_L(\mathbf{s}) \end{pmatrix} = \begin{pmatrix} \dfrac{\partial f(\mathbf{s}'; \mathbf{s})}{\partial x_1'} \\ \vdots \\ \dfrac{\partial f(\mathbf{s}'; \mathbf{s})}{\partial x_L'} \end{pmatrix}_{\mathbf{s}'=\mathbf{s}}, \tag{3}$$

is the dominant fitness component for the resident, the invading mutant replaces the resident to become a new resident. Hence, repeated mutant invasions induce directional evolution, and which is approximately described with an ordinary differential equation, called the canonical equation (Dieckmann and Law 1996):

$$\frac{d\mathbf{s}}{dt} = \frac{\mu \hat{n}}{2} \mathbf{V}_\mu \mathbf{g}(\mathbf{s}), \tag{4}$$

where μ describes the mutation rate per birth, and $\mathbf{V}_\mu$ is an $L \times L$ symmetric matrix describing the mutational covariance matrix. This directional evolution continues until the population comes close to a point $\mathbf{s}^*$ at which the fitness gradient vanishes,

$$\mathbf{g} = \mathbf{g}(\mathbf{s}^*) = \mathbf{0}, \tag{5}$$

called an evolutionarily singular point.

2.2 Convergence stability

When the resident phenotype $\mathbf{s}$ is close to $\mathbf{s}^*$, so that $\mathbf{g}(\mathbf{s}) = \mathbf{g}(\mathbf{s}^*) + \mathbf{C}^{\mathrm{T}}[\mathbf{s} - \mathbf{s}^*]$ approximately holds with

$$\mathbf{C} = \begin{pmatrix} \dfrac{\partial \mathbf{g}(\mathbf{s})^{\mathrm{T}}}{\partial x_1} \\ \vdots \\ \dfrac{\partial \mathbf{g}(\mathbf{s})^{\mathrm{T}}}{\partial x_L} \end{pmatrix}_{\mathbf{s}=\hat{\mathbf{s}}} = \begin{pmatrix} \dfrac{\partial g_1(\mathbf{s})}{\partial x_1} & \cdots & \dfrac{\partial g_L(\mathbf{s})}{\partial x_1} \\ \vdots & \ddots & \vdots \\ \dfrac{\partial g_1(\mathbf{s})}{\partial x_L} & \cdots & \dfrac{\partial g_L(\mathbf{s})}{\partial x_L} \end{pmatrix}_{\mathbf{s}=\mathbf{s}^*}, \tag{6}$$

we can transform Eq. (4) into

$$\frac{d\mathbf{s}}{dt} = \frac{\mu \hat{n}}{2} \mathbf{V}_\mu \mathbf{C}^{\mathrm{T}}[\mathbf{s} - \mathbf{s}^*]. \tag{7}$$

Based on this equation, the three classes of convergence stability are described as follows (Leimar 2009). First, $\mathbf{s}^*$ is convergence stable, when all eigenvalues of $\mathbf{V}_\mu \mathbf{C}^{\mathrm{T}}$ have negative real parts, expressed as

$$\lambda_{\max}(\mathbf{C}\mathbf{V}_\mu) < 0, \tag{8}$$

(because $\lambda_{\max}(\mathbf{V}_\mu \mathbf{C}^{\mathrm{T}}) = \lambda_{\max}\left([\mathbf{V}_\mu \mathbf{C}^{\mathrm{T}}]^{\mathrm{T}}\right) = \lambda_{\max}(\mathbf{C}\mathbf{V}_\mu)$ holds), where $\lambda_{\max}(\circ)$ gives the largest value among real parts of the eigenvalues for a matrix $\circ$. Eq. (8) ensures the

convergence of $\mathbf{s}$ toward $\mathbf{s}^*$ through the directional evolution described with Eq. (7), under the specific mutational covariance matrix, $\mathbf{V}_\mu$. Second, $\mathbf{s}^*$ is *strongly* convergence stable, when all eigenvalues of the symmetric part of $\mathbf{C}$ are negative (i.e., $[\mathbf{C}+\mathbf{C}^{\mathrm{T}}]/2$ is negative definite), expressed as

$$\lambda_{\max}\left(\frac{\mathbf{C}+\mathbf{C}^{\mathrm{T}}}{2}\right) < 0, \tag{9}$$

and which ensures the convergence of $\mathbf{s}$ toward $\mathbf{s}^*$ under any regular $\mathbf{V}_\mu$ through the directional evolution described with Eq. (7). Third, $\mathbf{s}^*$ is *absolutely* convergence stable, when $\mathbf{C}$ is symmetric and its eigenvelus are all negative, expressed as

$$\mathbf{C}^{\mathrm{T}} = \mathbf{C} \quad \text{and} \quad \lambda_{\max}(\mathbf{C}) < 0, \tag{10}$$

ensuring the convergence of $\mathbf{s}$ toward $\mathbf{s}^*$ under any sequences of possible mutant invasions. Note that all absolutely convergence stable points are included in strongly convergence stable points, i.e., Eq. (10) is sufficient for Eq. (9), and that all strongly convergence stable points are included in convergence stable points, i.e., Eq. (9) is sufficient for Eq. (8).

2.3 Evolutionary stability

The singular point $\mathbf{s}^*$ is (locally) evolutionarily stable, i.e., any mutant in the neighborhood of $\mathbf{s}^*$ cannot invade the resident placed at $\mathbf{s}^*$, if the symmetric matrix

$$\mathbf{D} = \begin{pmatrix} \dfrac{\partial^2 f(\mathbf{s}',\mathbf{s})}{\partial x_1'^2} & \cdots & \dfrac{\partial^2 f(\mathbf{s}',\mathbf{s})}{\partial x_1' \partial x_L'} \\ \vdots & \ddots & \vdots \\ \dfrac{\partial^2 f(\mathbf{s}',\mathbf{s})}{\partial x_L' \partial x_1'} & \cdots & \dfrac{\partial^2 f(\mathbf{s}',\mathbf{s})}{\partial x_L' \partial x_L'} \end{pmatrix}_{\mathbf{s}'=\mathbf{s}=\mathbf{s}^*} \tag{11}$$

has only negative eigenvalues. Conversely, $\mathbf{s}^*$ is evolutionarily unstable if the maximum eigenvalue of $\mathbf{D}$ is positive, expressed as

$$\lambda_{\max}(\mathbf{D}) > 0. \tag{12}$$

2.4 Evolutionary branching points

According to Doebeli (2011), the requirements for a point $\mathbf{s}^*$ being an evolutionary branching point are described as follows:

(i) $\mathbf{s}^*$ is convergence stable.
(ii) $\mathbf{s}^*$ is evolutionarily unstable in at least one direction of trait space.
(iii) Mutual invasibility (i.e., $f(\mathbf{s}';\mathbf{s}) > 0$ and $f(\mathbf{s};\mathbf{s}') > 0$) holds around $\mathbf{s}^*$ in the directions of evolutionary instability given by (ii).
(iv) The different phenotypic branches constituting the protected polymorphism given by (iii) diverge evolutionarily from $\mathbf{s}^*$.

In one-dimensional trait spaces, (i) and (ii) are sufficient for (iii) and (iv) (Metz et al. 1996; Geritz et al. 1997). In the higher-dimensional trait spaces, (i) and (ii) are not sufficient for (iii) and (iv). Moreover, (i-iii) may not be sufficient for (iv) (Doebeli 2011; Geritz et al. 2016).

3 Result

In this section, we describe our developed conditions for the branching possibility and

branching inevitability in association with (i-iv) in Section 2.4. Then, we show whether the three classes of convergence stable points may have either or both the branching possibility and inevitability.

3.1 Approximate fitness function

Following Meszéna (2005), we approximate the fitness for phenotype $\mathbf{s}'$ under coexisting phenotypes $\mathbf{s}_1, \dots, \mathbf{s}_M$ in the neighborhood of an evolutionarily singular point $\hat{\mathbf{s}}$ as a quadratic function of $\mathbf{s}'$:

$$F\big(\mathbf{s}'; (\mathbf{s}_1, \dots, \mathbf{s}_M), (n_1, \dots, n_M)\big) = [\bar{\mathbf{s}} - \mathbf{s}^*]^{\mathrm{T}}\mathbf{C}[\mathbf{s}' - \bar{\mathbf{s}}] + \frac{1}{2}[\mathbf{s}' - \bar{\mathbf{s}}]^{\mathrm{T}}\mathbf{D}[\mathbf{s}' - \bar{\mathbf{s}}] - \frac{1}{2}V_{\mathbf{D}} + \bar{F} \quad (13)$$

(see Appendix S1 for the derivation), where $\bar{\mathbf{s}} = \sum_{i=1}^{M} p_i \mathbf{s}_i$ and $\bar{F} = \sum_{i=1}^{M} p_i F(\mathbf{s}_i; (\mathbf{s}_1, \dots, \mathbf{s}_M), (n_1, \dots, n_M))$ with $p_i = n_i / \sum_{j=1}^{M} n_j$ are respectively the average phenotype and the average fitness among the coexisting phenotypes, and where $V_{\mathbf{D}} = \sum_{j=1}^{M} p_j \left[\mathbf{s}_j - \bar{\mathbf{s}}\right]^{\mathrm{T}} \mathbf{D}\left[\mathbf{s}_j - \bar{\mathbf{s}}\right]$ is the variance weighted with $\mathbf{D}$. From Eq. (13) the following results are obtained.

3.2 Branching possibility

As shown in Appendix S2, the following proposition holds good:

> If an evolutionarily singular point $\mathbf{s}^*$ satisfies the branching possibility conditions defined below, then $\mathbf{s}^*$ has a *branching possibility* in the sense that there is a non-zero probability of eventual evolutionary branching for an arbitrary monomorphic resident $\mathbf{s}$ in the neighborhood of $\mathbf{s}^*$, through trait substitution sequences consisting of deterministic convergence of a monomorphic resident toward $\mathbf{s}^*$ (monomorphic convergence), probabilistic emergence of dimorphism and their initial divergence, and their deterministic divergence through directional evolution (dimorphic divergence).

Branching possibility conditions:

$$\begin{aligned}
&\lambda_{\max}(\mathbf{C}\mathbf{V}_\mu) < 0 && \text{(convergence stability)},\\
&\lambda_{\max}(\mathbf{D}) > 0 && \text{(evolutionary instability)},\\
&\mathbf{e}^{\mathrm{T}}[\mathbf{D} - \mathbf{C}]\mathbf{e} > 0 && \text{(dimorphic emergence: mutual invasibility)},\\
&\lambda_{\max}(\mathbf{C}_{\mathrm{d}}\mathbf{V}_\mu) < \frac{\mathbf{e}^{\mathrm{T}}\mathbf{D}\mathbf{e}}{\mathbf{e}^{\mathrm{T}}\mathbf{V}_\mu^{-1}\mathbf{e}} && \text{(locally stable dimorphic divergence)},
\end{aligned} \quad (14)$$

$$\mathbf{C}_{\mathrm{d}} = \mathbf{C} + \frac{\mathbf{C}\mathbf{e}\mathbf{e}^{\mathrm{T}}\mathbf{C}}{\mathbf{e}^{\mathrm{T}}[\mathbf{D} - \mathbf{C}]\mathbf{e}},$$

where $\mathbf{e}$ is a unit vector describing the direction of dimorphic divergence, given by

$$\begin{aligned}
\mathbf{e} &= \frac{\mathbf{v}_{\mathbf{D}}}{|\mathbf{v}_{\mathbf{D}}|},\\
\mathbf{v}_{\mathbf{D}} &= \sqrt{\mathbf{V}_\mu}^{\mathrm{T}}\, \mathbf{v}_{\lambda\max}\left(\sqrt{\mathbf{V}_\mu}\mathbf{D}\sqrt{\mathbf{V}_\mu}^{\mathrm{T}}\right),
\end{aligned} \quad (15)$$

where $\mathbf{v}_{\lambda\max}(\circ)$ gives the eigenvector for the $\lambda_{\max}(\circ)$ for a matrix $\circ$, and $\sqrt{\mathbf{V}_\mu}$ is an $L \times L$

matrix satisfying $\sqrt{\mathbf{V}_\mu}^{\mathrm{T}}\sqrt{\mathbf{V}_\mu} = \mathbf{V}_\mu$ (given by $\sqrt{\mathbf{V}_\mu} = \mathrm{diag}\left(\sqrt{\lambda_{\mu 1}}, \dots, \sqrt{\lambda_{\mu L}}\right)\left(\mathbf{v}_{\mu 1}, \dots, \mathbf{v}_{\mu L}\right)^{\mathrm{T}}$, where $\lambda_{\mu 1}, \dots, \lambda_{\mu L}$ and $\mathbf{v}_{\mu 1}, \dots, \mathbf{v}_{\mu L}$ are the eigenvalues and their eigenvectors of $\mathbf{V}_\mu$, and where $\mathrm{diag}\left(\sqrt{\lambda_{\mu 1}}, \dots, \sqrt{\lambda_{\mu L}}\right)$ is the diagonal matrix with its entries $\sqrt{\lambda_{\mu 1}}, \dots, \sqrt{\lambda_{\mu L}}$). Note that the four inequalities in Eq. (14) respectively correspond to (i-iv) in Section 2.4.

The fourth inequality in Eq. (14), "locally stable dimorphic divergence," ensures steady progress of diversifying directional evolution of coexisting two monomorphic populations described with the canonical equation, once the two residents have sufficiently diverged from each other along the direction of $\mathbf{e}$ with their positions being approximately symmetric about $\mathbf{s}^*$. (i.e., for the directionally evolving two populations with their phenotypes denoted by $\mathbf{s}_1$ and $\mathbf{s}_2$, the dynamics of $\mathbf{u} = [\mathbf{s}_1 - \mathbf{s}_2]/\Delta z - \mathbf{e}$ and $\mathbf{w} = [\mathbf{s}_1 + \mathbf{s}_2]/[2\Delta z]$ with $\Delta z = \left|\mathbf{e}^{\mathrm{T}}[\mathbf{s}_1 - \mathbf{s}_2]\right|$ has a locally stable fixed point $(\mathbf{u}, \mathbf{w}) = (0,0)$ under Eq. (14), as derived in Appendix S2.3).

Figure 1 shows evolutionary branching in numerically simulated evolution (i.e., trait substitution sequences calculated under Eq. (13) following Ito and Sasaki (2020, 2023)) for an initially monomorphic population around $\mathbf{s}^*$ satisfying the branching possibility conditions. The dynamics of evolutionary branching shown in Fig.1 are kept qualitatively similar even in the individual-based stochastic simulation under the assumption of non-rare mutation (and asexual reproduction), as shown in Figure 2.

3.3 Branching inevitability

As shown in Appendix S3, the following proposition holds good:

> If an evolutionarily singular point $\mathbf{s}^*$ satisfies the branching inevitability conditions defined below, then $\mathbf{s}^*$ has a *branching inevitability* in the sense that $\mathbf{s}^*$ has a local Lyapunov function ensuring the inevitable and deterministic progress of evolutionary branching for an arbitrary monomorphic resident $\mathbf{s}$ in the neighborhood of $\mathbf{s}^*$.

Branching inevitability conditions:

$$\begin{aligned} &\mathbf{C}^{\mathrm{T}} = \mathbf{C} \quad \text{and} \quad \lambda_{\max}(\mathbf{C}) > 0 && \text{(absolute convergence stability)}, \\ &\lambda_{\max}(\mathbf{D}) > 0 && \text{(evolutionary instability)}. \end{aligned} \tag{16}$$

Note that all absolutely convergence stable non-ESSes have the branching inevitability, because there exists a local Lyapunov function H given by

$$\begin{aligned} H &= H_C + H_D, \\ H_C &= [\bar{\mathbf{s}} - \mathbf{s}^*]^{\mathrm{T}}\mathbf{C}[\bar{\mathbf{s}} - \mathbf{s}^*], \\ H_D &= \sum_{j=1}^{M} p_j \left[\mathbf{s}_j - \bar{\mathbf{s}}\right]^{\mathrm{T}}\mathbf{D}\left[\mathbf{s}_j - \bar{\mathbf{s}}\right] = V_{\mathbf{D}}, \end{aligned} \tag{17}$$

where H_C is a distance measure for $\bar{\mathbf{s}}$ from the $\mathbf{s}^*$ weighted with $\mathbf{C}$, whereas H_D is a variance measure weighted with $\mathbf{D}$ for the coexisting phenotypes. Note that $H_C \leq 0$ always holds under Eq. (16). As derived in Appendix S3, the time derivative of H satisfies

$$\frac{dH}{dt} = 2\sum_{i=1}^{M} p_i[F_i - \bar{F}]^2 \geq 0, \tag{18}$$

where $F_i = F(\mathbf{s}_i; (\mathbf{s}_1, \dots, \mathbf{s}_M), (n_1, \dots, n_M))$ is the fitness for the ith phenotype, and $\bar{F} = \sum_{i=1}^{M} p_i F_i$ is the average fitness among them (see also Eq. (13)). $dH/dt = 0$ holds only when the population dynamics completely stops.

When directional evolution of a monomorphic population converges toward a point $\mathbf{s}^*$ that satisfies the branching inevitability conditions, $|H_D|$ is kept very small and hence the increase of H is realized by the monotonic increase of H_C toward zero (orange dotted curve in the right panel of Fig. 1c). In contrast, after sufficient convergence of the population toward $\mathbf{s}^*$, the increase of H is realized by the increase of H_D that corresponds to the emergence of polymorphism and their divergent evolution (green dotted curve in the right panel of Fig. 1c).

3.4 Branching possibility and inevitability for three classes of convergence stable non-ESSes

Table 1 shows whether convergence stable non-ESSes of each convergence class can have either the branching possibility or inevitability, or both (see Appendix S4 for the derivation).

	Convergence stable non-ESS	Strongly convergence stable non-ESS	Absolutely convergence stable non-ESS
Evolutionary singularity	$\mathbf{g} = \mathbf{0}$	$\mathbf{g} = \mathbf{0}$	$\mathbf{g} = \mathbf{0}$
Convergence stability	$\lambda_{\max}(\mathbf{C}\mathbf{V}_\mu) < 0$	$\lambda_{\max}([\mathbf{C} + \mathbf{C}^{\mathrm{T}}]/2) < 0$	$\mathbf{C} = \mathbf{C}^{\mathrm{T}}, \lambda_{\max}(\mathbf{C}) < 0$
Evolutionary instability	$\lambda_{\max}(\mathbf{D}) > 0$	$\lambda_{\max}(\mathbf{D}) > 0$	$\lambda_{\max}(\mathbf{D}) > 0$
Additional conditions (for dimorphic emergence and locally stable dimorphic divergence)	$\mathbf{e}^{\mathrm{T}}[\mathbf{D} - \mathbf{C}]\mathbf{e} > 0$ $\lambda_{\max}(\mathbf{C}_{\mathrm{d}}\mathbf{V}_\mu) < \frac{\mathbf{e}^{\mathrm{T}}\mathbf{D}\mathbf{e}}{\mathbf{e}^{\mathrm{T}}\mathbf{V}_\mu^{-1}\mathbf{e}}$ (only for $L \geq 3$)	Not required	Not required
Branching possibility	YES	YES	YES
Branching inevitability	?	?	YES
Class of evolutionary branching point	Possible branching point	Strongly possible branching point	Inevitable branching point

Table 1. Three classes of convergence stable non-ESSes in an arbitrary L-dimensional trait spaces ($L \geq 2$) and their branching possiblity (Eq. (14)) and branching inevitability (Eq. (16)). $\lambda_{\max}(\cdot)$ is the largest value among real parts of the eigenvalues for $\cdot$, and $\mathbf{e}$ is the direction of the dimorphic divergence (Eq. (15)).

As shown in Table 1, the branching possibility is warranted for convergence stable non-ESSes satisfying the two additional conditions for dimorphic emergence and locally stable dimorphic divergence, and hence they are referred to as "possible branching points." Note that there can exist possible branching points that are not strongly convergence stable. Such possible branching points can induce evolutionary branching composed of spiral monomorphic convergence followed by linear dimorphic divergence (Figs. 1a, 2a). Note also that in two-

dimensional trait spaces the first additional condition (i.e., the condition for dimorphic emergence, $\mathbf{e}^{\mathrm{T}}[\mathbf{D}-\mathbf{C}]\mathbf{e} > 0$) is sufficient for the second additional condition. This relationship does not hold in the higher-dimensional trait spaces, in which case it is possible that the first additional condition is satisfied but not the second, implying that dimorphic divergence can start but may collapse eventually (Fig. 3).

Regarding strongly convergence stable non-ESSes, they have the branching possibility under any regular $\mathbf{V}_\mu$ without the additional conditions, and hence they are referred to as "strongly possible branching points" (Figs.1b and 2b). Regarding absolutely convergence stable non-ESSes, they have both the branching possibility and inevitability under any regular $\mathbf{V}_\mu$ without the additional conditions, and hence they are referred to as "inevitable branching points" (Figs. 1c and 2c).

3.5 Quantitative index for branching possibility

Because what the branching possibility conditions ensure is not a high probability but a non-zero probability for evolutionary branching (Eq. S2.11 in Appendix S2.1), the probability for evolutionary branching under some possible or strongly possible branching points could be extremely low. Indeed, when the imaginary parts of the eigenvalues of $\mathbf{C}$ have much larger magnitudes than the real parts, numerically simulated evolution tends to show monomorphic directional evolution that orbit around the possible branching point for extremely large numbers of invasions without occurrence of evolutionary branching. For a simple example, a point $\mathbf{s}^*$ with

$$\mathbf{C} = \begin{pmatrix} -a & -1 \\ 1 & -a \end{pmatrix}, \mathbf{D} = \begin{pmatrix} a & 0 \\ 0 & -a \end{pmatrix}, \mathbf{V}_\mu = \sigma^2 \begin{pmatrix} 1 & 0 \\ 0 & 1 \end{pmatrix} \tag{19}$$

with a and σ being positive constants is a strongly possible branching point (where σ describes the average mutational step size and is assumed to satisfy $0 < \sigma \ll 1$). However, when a is much smaller than 1, the monomorphic directional evolution tends to show a circular orbit around $\mathbf{s}^*$ characterized with a circle with its radius σ/a being much larger than σ (Fig. 4d; see Appendix S5). In this case, the population is kept away from $\mathbf{s}^*$ so that the emergence of dimorphism and their divergence are extremely unlikely, despite that $\mathbf{s}^*$ is a strongly possible branching point (Fig. 4a-b).

To roughly estimate the likelihood of evolutionary branching for possible branching points, a sufficient condition for the emergence of dimorphism (along $\mathbf{e}$ during directional evolution in the circular orbit around $\mathbf{s}^*$) is approximately derived in Appendix S5 as

$$Q = \frac{\mathbf{e}^{\mathrm{T}}[\mathbf{D}-\mathbf{C}]\mathbf{e}}{\mathbf{e}^{\mathrm{T}}\mathbf{V}_\mu^{-1}\mathbf{e}} \min_i \left(\frac{|\mathrm{Re}(\lambda_i)|}{\mathrm{Re}(\lambda_i)^2 + \mathrm{Im}(\lambda_i)^2} \right) > 1 \tag{20}$$

with λ_i describing the ith eigenvalue of $\mathbf{C}\mathbf{V}_\mu$. On this basis, we may expect a high likelihood of evolutionary branching when $Q > 1$ holds. For example, Eq. (19) gives $Q = 2a^2/[1+a^2]$. As far as numerically examined, Q seems useful as a quantitative index for the likelihood of evolutionary branching in simulated evolution as trait substitution sequences (Fig. 4c and Fig. 5).

4 Application example

We show a simple application example for the conditions for possible, strongly possible, and

inevitable branching points, developed in the previous section. We consider a two-dimensional trait space $\mathbf{s} = (x, y)^{\mathrm{T}}$ for describing the phenotypes of a cannibalistic population, where individuals prey not only on other kinds of organisms as their main resource but also on themselves. Trait x describes the trait as predator or consumer (e.g., mouth size), and trait y describes the trait as prey or resource (e.g., body size), as is common in aquatic carnivores. For simplicity, we assume isotropic mutation such that $\mathbf{V}_\mu = \sigma^2\mathbf{I}$ holds. For arbitrary M coexisting phenotypes $\mathbf{s}_1, \dots, \mathbf{s}_M$ with their population sizes $n_1, \dots, n_M$, we define their population dynamics as

$$\begin{aligned}\frac{1}{n_i}\frac{dn_i}{dt} &= F(\mathbf{s}_i; (\mathbf{s}_1, \dots, \mathbf{s}_M), (n_1, \dots, n_M)) \\ &= \left[r(x_i, y_i) - \sum_{j=1}^{M} \alpha(x_i - x_j) n_j\right] + c\left[\rho \sum_{j=1}^{M} \beta(x_i - y_j) n_j - \sum_{j=1}^{M} \beta(x_j - y_i) n_j\right]. \quad (21)\end{aligned}$$

Here, $r(x_i, y_i)$ describes the intrinsic growth rate for the ith phenotype deriving from the main resource in the absence of competitors, which is defined for simplicity as $r(x_i, y_i) = 1 + \frac{1}{2} r_{xx} x_i^2 + \frac{1}{2} r_{yy} y_i^2$ with constants r_{xx} and r_{yy}. $\alpha(x_i - x_j)$ describes the negative interaction between the ith and jth phenotypes through competition for the main resource. $\beta(x_i - y_j)$ describes the predation amount by the ith phenotype on the jth phenotype per unit population sizes for them (corresponding to type-I functional response). A constant c describes the amount of cannibalistic interaction relative to that of resource competition for the main resource, and a constant ρ describes the assimilation rate for the resource intake from the cannibalistic interaction. We define $\alpha(x)$ and $\beta(x)$ as

$$\alpha(x) = \exp\left(-\frac{x^2}{2\sigma_\alpha^2}\right), \beta(x) = \exp\left(-\frac{x^2}{2\sigma_\beta^2}\right), \quad (22)$$

with σ_α and σ_β describing the widths of resource competition and cannibalistic interaction, respectively.

When there exists a single resident $\mathbf{s} = (x, y)^{\mathrm{T}}$, its equilibrium population size is given by

$$\hat{n} = \frac{r(x, y)}{1 + c[1 + \rho]\beta(x - y)}. \quad (23)$$

The invasion fitness for a mutant $\mathbf{s}' = (x', y')^{\mathrm{T}}$ against resident $\mathbf{s} = (x, y)^{\mathrm{T}}$ is derived as

$$\begin{aligned}f(\mathbf{s}'; \mathbf{s}) &= \lim_{n' \to 0} F\big(\mathbf{s}'; (\mathbf{s}', \mathbf{s}), (n', \hat{n})\big) \\ &= 1 + \frac{1}{2} r_{xx} x'^2 + \frac{1}{2} r_{yy} y'^2 + [-\alpha(x' - x) + \rho c \beta(x' - y) - c\beta(x - y')]\hat{n}. \quad (24)\end{aligned}$$

Then from the fitness gradient for the resident, given by

$$\begin{aligned}g_x(x, y) &= \left[\frac{\partial f}{\partial x'}\right]_{\mathbf{s}'=\mathbf{s}} = r_{xx} x - \frac{\rho c \hat{n}}{\sigma_\beta^2}[x - y]\beta(x - y), \\ g_y(x, y) &= \left[\frac{\partial f}{\partial y'}\right]_{\mathbf{s}'=\mathbf{s}} = r_{yy} y - \frac{c \hat{n}}{\sigma_\beta^2}[x - y]\beta(x - y), \quad (25)\end{aligned}$$

we find an evolutionarily singular point at the origin, i.e., $\mathbf{s}^* = (0,0)^{\mathrm{T}}$. By applying Eqs. (6) and (11) for $\mathbf{s}^* = (0,0)^{\mathrm{T}}$, we obtain

$$\mathbf{C} = \begin{pmatrix} C_{xx} & C_{xy} \\ C_{yx} & C_{yy} \end{pmatrix} = \begin{pmatrix} r_{xx} - c\rho A & -cA \\ c\rho A & r_{yy} + cA \end{pmatrix},$$

$$\mathbf{D} = \begin{pmatrix} D_{xx} & D_{xy} \\ D_{xy} & D_{yy} \end{pmatrix} = \begin{pmatrix} r_{xx} + \left[\frac{\sigma_\beta^2}{\sigma_\alpha^2} - c\rho\right] A & 0 \\ 0 & r_{yy} + cA \end{pmatrix}, \tag{26}$$

where $A = \hat{n} \,/\, \sigma_\beta^2$ is always positive. Then, the condition for $\mathbf{s}^*$ being convergence stable under isotropic mutation, i.e., $\lambda_{\max}(\mathbf{C}) < 0$, is expressed as

$$\begin{aligned} \lambda_1 \lambda_2 &= C_{xx} C_{yy} - C_{xy} C_{yx} > 0, \\ \lambda_1 + \lambda_2 &= C_{xx} + C_{yy} < 0. \end{aligned} \tag{27}$$

The condition for $\mathbf{s}^*$ being strongly convergence stable, i.e., $\lambda_{\max}(\mathbf{C}^{\mathrm{str}}) < 0$ with $\mathbf{C}^{\mathrm{str}} = [\mathbf{C} + \mathbf{C}^{\mathrm{T}}]/2$, is expressed as

$$\begin{aligned} \lambda_1^{\mathrm{str}} \lambda_2^{\mathrm{str}} &= C_{xx} C_{yy} - \frac{\left[C_{xy} + C_{yx}\right]^2}{4} > 0, \\ \lambda_1^{\mathrm{str}} + \lambda_2^{\mathrm{str}} &= C_{xx} + C_{yy} < 0. \end{aligned} \tag{28}$$

The conditions for $\mathbf{s}^*$ being absolutely convergence stable, i.e., $\mathbf{C}^{\mathrm{T}} = \mathbf{C}$ and $\lambda_{\max}(\mathbf{C}) < 0$, are expressed as

$$\begin{aligned} c &= 0, \\ \lambda_1^{\mathrm{abs}} \lambda_2^{\mathrm{abs}} &= C_{xx} C_{yy} > 0, \\ \lambda_1^{\mathrm{abs}} + \lambda_2^{\mathrm{abs}} &= C_{xx} + C_{yy} < 0. \end{aligned} \tag{29}$$

Regarding evolutionary stability, the condition for $\mathbf{s}^*$ being evolutionarily unstable can be expressed as

$$\lambda_{\max}(\mathbf{D}) = \max\{D_{xx}, D_{yy}\} = \max\left\{C_{xx} + \frac{\sigma_\beta^2}{\sigma_\alpha^2} A, C_{yy}\right\} > 0. \tag{30}$$

Here, for the simplicity, we assume that $D_{yy} = C_{yy} = r_{yy} + cA < 0$ always holds. In this case, the direction of dimorphic divergence is obtained from Eq. (15) as the eigenvector $\mathbf{e} = (1,0)^{\mathrm{T}}$ for $\lambda_{\max}(\mathbf{D}) = D_{xx} = C_{xx} + \frac{\sigma_\beta^2}{\sigma_\alpha^2} A$.

The condition for $\hat{\mathbf{s}}$ being a possible branching point is given by Eqs. (27) and (30), because the additional condition,

$$\mathbf{e}^{\mathrm{T}}[\mathbf{D} - \mathbf{C}]\mathbf{e} > 0, \tag{31}$$

is always satisfied when Eq. (30) holds (i.e., $\mathbf{e}^{\mathrm{T}}[\mathbf{D} - \mathbf{C}]\mathbf{e} = D_{xx} - C_{xx} = \frac{\sigma_\beta^2}{\sigma_\alpha^2} A > 0$). The conditions for $\mathbf{s}^*$ for being a strongly possible branching point are given by Eq. (28) and (30). The conditions for $\mathbf{s}^*$ for being an inevitable branching point are given by Eq. (29) and (30). The dependency of these branching point conditions on r_{xx}, r_{yy}, and c is shown in Figure 6. Numerically simulated evolutionary branchings induced by these branching points are shown in Figures 7 and 8. Notably, we see from Eqs. (26-30) that $\mathbf{s}^*$ is a possible branching point that is not a strongly possible branching point (and hence not an inevitable branching point) when $\mathbf{s}^*$ satisfies

$$c^2\rho A^2 < [r_{xx} - \mathrm{c}\rho A][r_{yy} + cA] < \frac{c^2[1-\rho]^2 A^2}{4},$$
$$r_{xx} + r_{yy} < -\mathrm{c}[1-\rho]A,$$
$$r_{xx} > \left[\mathrm{c}\rho - \frac{\sigma_\beta^2}{\sigma_\alpha^2}\right]A. \tag{32}$$

In this case, the numerically simulated evolutionary branching typically shows the spiral trajectory of monomorphic convergence followed by the linear trajectories of dimorphic divergence (Figs. 7a and 8a, analogously to Figs.1a and 2a). Notably, evolutionary branching can be induced by possible branching points that lack convergence stability along the x-direction, i.e., $C_{xx} = r_{xx} - c\rho A < 0$ (Figs. 7a and 8a, which are similar to Figs. 1a and 2a).

Notably also, in Figure 6, a large c (i.e., strength of cannibalistic interaction relative to the resource competition) gives a large parameter region for possible branching points that are not strongly possible branching point. This is because a large c causes a large $|C_{xy} - C_{yx}|$ through the interactions in the fitness function between mutant's trait x and resident's trait y and between mutant's trait y and resident's trait x. In general, this kind of relationship can be expected when two different kinds of traits interactively contribute to the fitness function so that $\left|C_{xy} - C_{yx}\right| = \left|\frac{\partial^2 f(\mathbf{s}';\mathbf{s})}{\partial x' \partial \mathrm{y}} - \frac{\partial^2 f(\mathbf{s}';\mathbf{s})}{\partial y' \partial x}\right|_{\mathbf{s}'=\mathbf{s}}$ is large (e.g., the contribution of weapons and armors in fighting for territorires, and that of optical and sonic sensors and their target signals in mating).

5 Discussion

For one-dimensional trait spaces, the likelihood of evolutionary branching for a monomorphic population is well characterized by whether the spaces have convergence stable non-ESSes, called evolutionary branching points (Metz et al. 1996; Geritz et al. 1997). For trait spaces with arbitrary higher dimensions, however, evolutionary branching points have not been formally extended yet. So far, strongly convergence stable non-ESSes have been treated as the candidates for evolutionary branching points (Ackermann and Doebeli 2004; Ito and Shimada 2007; Ito and Dieckmann 2012, 2014; Geritz et al. 2016; Ito and Sasaki 2016, 2020).

Geritz et al. (2016) described the initial divergent evolution of polymorphic residents (emerged in the neighborhood of convergence stable non-ESSes) with the coupled Lande's equations (Lande 1979), under assumption that the timescales of population dynamics and evolutionary dynamics are not separated. They derived a set of conditions ensuring that the initial divergent evolution of slightly differentiated morphs in trait spaces of arbitrary dimensions result in dimorphic divergence without collapse into a single morph. While these conditions are satisfied by strongly convergence stable non-ESSes in two-dimensional trait spaces, the higher-dimensional cases remain to be analyzed further (Geritz et al. 2016). In addition, the progress of their divergent evolution eventually causes strong selection gradients on them so that the canonical equation becomes the more suitable descriptor for the dynamics, but the conditions for stable progress of the divergent evolution described with the canonical equation have not been obtained.

In the present study, we analyzed in trait spaces of arbitrary dimension whether convergence stable non-ESSes can induce evolutionary branching, by examining the branching possibility (based on the canonical equation) and the branching inevitability (based on the local Lyapunov

function). In this study, dimorphic divergence is described with the canonical equations, and which gives a more straightforward connection with trait substitution sequences in adaptive dynamics theory than describing it with the Lande's equations (Geritz et al. 2016). Instead, the dependency of the canonical equations on population sizes makes the analysis difficult. To reduce this difficulty, we focused not on global but on local stability for the progress of dimorphic divergence, and which enabled derivation of the branching possibility condition that can easily be examined for trait spaces of arbitrary dimensions. (Our obtained conditions for the locally stable dimorphic divergence are different from but structurally similar to the conditions derived by Geritz et al. (2016).)

Consequently, for trait spaces of arbitrary dimensions, we showed that the branching possibility is warranted not only for strongly convergence-stable non-ESSes, but also for convergence-stable non-ESSes that are not strongly convergence stable, as long as these points satisfy the conditions for the emergence of dimorphism and their locally stable divergence (Table 1). This analytical result showed good agreement with likelihoods of evolutionary branching in numerically simulated evolution. However, the branching possibility conditions are qualitative conditions in the sense that they only ensure non-zero probability for evolutionary branching. The quantitative prediction for the branching likelihood might be developed by formal derivation and improvement of our heuristically developed index, Eq. (20).

We also showed that all absolutely convergence stable non-ESSes satisfy the branching inevitability condition; they have local Lyapunov functions ensuring steady progress of evolutionary branching even without timescale separation between population dynamics and evolutionary dynamics. This implies that dynamics of evolutionary branching can be considerably deterministic. Moreover, absolute convergence stable points may be more common among eco-evolutionary models than previously thought (Leimar 2009), because convergence stable points are always absolutely convergence stable in an arbitrary trait space consisting of a trait under frequency-dependent selection and of one or more traits under frequency-independent selection (as in the application example in Section 4 with $c = 0$).

References

Ackermann M, Doebeli M (2004) Evolution of Niche Width and Adaptive Diversification. Evolution 58:2599–2612. https://doi.org/10.1111/j.0014-3820.2004.tb01614.x

Dieckmann U, Doebeli M, Metz JAJ, Tautz D (eds) (2004) Adaptive Speciation. Cambridge University Press, Cambridge

Dieckmann U, Law R (1996) The dynamical theory of coevolution: a derivation from stochastic ecological processes. J Math Biol 34:579–612

Doebeli M (2011) Adaptive Diversification. Princeton University Press

Doebeli M, Ispolatov I (2010) Complexity and Diversity. Science 328:494–497. https://doi.org/10.1126/science.1187468

Eshel I (1983) Evolutionary and continuous stability. J Theor Biol 103:99–111. https://doi.org/10.1016/0022-5193(83)90201-1

Geritz SAH, Metz JAJ, Kisdi É, Meszéna G (1997) Dynamics of Adaptation and Evolutionary Branching. Phys Rev Lett 78:2024–2027. https://doi.org/10.1103/PhysRevLett.78.2024

Geritz SAH, Metz JAJ, Rueffler C (2016) Mutual invadability near evolutionarily singular strategies for multivariate traits, with special reference to the strongly convergence stable case. J Math Biol 72:1081–1099. https://doi.org/10.1007/s00285-015-0944-6

Ito H, Sasaki A (2016) Evolutionary branching under multi-dimensional evolutionary constraints. J Theor Biol 407:409–428. https://doi.org/10.1016/j.jtbi.2016.07.011

Ito HC, Dieckmann U (2012) Evolutionary-branching lines and areas in bivariate trait spaces. Evol Ecol Res 14:555–582

Ito HC, Dieckmann U (2014) Evolutionary branching under slow directional evolution. J Theor Biol 360:290–314. https://doi.org/10.1016/j.jtbi.2013.08.028

Ito HC, Dieckmann U (2007) A new mechanism for recurrent adaptive radiations. Am Nat 170:E96–E111

Ito HC, Dieckmann U, Metz JAJ (2020) Lotka–Volterra approximations for evolutionary trait-substitution processes. J Math Biol 80:2141–2226. https://doi.org/10.1007/s00285-020-01493-y

Ito HC, Sasaki A (2020) Evolutionary branching in distorted trait spaces. J Theor Biol 489:110152. https://doi.org/10.1016/j.jtbi.2020.110152

Ito HC, Sasaki A (2023) The Adaptation Front Equation Explains Innovation-Driven Taxonomic Turnovers and Living Fossilization. Am Nat 202:E163–E180. https://doi.org/10.1086/727046

Ito HC, Shimada M (2007) Niche expansion: coupled evolutionary branching of niche position and width. Evol Ecol Res 9:675–695

Lande R (1979) Quantitative genetic analysis of multivariate evolution, applied to brain: body size allometry. Evolution 33:402–416

Leimar O (2009) Multidimensional convergence stability. Evol Ecol Res 11:

Maynard Smith J, Price GR (1973) The Logic of Animal Conflict. Nature 246:15–18. https://doi.org/10.1038/246015a0

Meszéna G, Gyllenberg M, Jacobs FJ, Metz JAJ (2005) Link between Population Dynamics and Dynamics of Darwinian Evolution. Phys Rev Lett 95:078105. https://doi.org/10.1103/PhysRevLett.95.078105

Metz JAJ, Geritz SAH, Meszéna G, et al (1996) Adaptive dynamics, a geometrical study of the consequences of nearly faithful reproduction. Stochastic and spatial structures of dynamical systems. In: van Strien SJ, Verduyn Lunel SM (eds) Stochastic and spatial structures of dynamical systems. North Holland, Amsterdam, pp 183–231

Schluter D (2000) The Ecology of Adaptive Radiation. Oxford University Press, Oxford, New York

Vukics A, Asbóth J, Meszéna G (2003) Speciation in multidimensional evolutionary space. Phys Rev E 68:041903. https://doi.org/10.1103/PhysRevE.68.041903

Figure legends

Figure 1

Numerically simulated evolutionary branching in a two-dimensional trait space, $\mathbf{s} = (x, y)^{\mathrm{T}}$, induced by a possible branching point (a), strongly possible branching point (b), or inevitable branching point (c), which respectively correspond to convergence stable, strongly convergence stable, and absolute convergence stable non-ESSes. Thin blue curves indicate evolutionary trajectories simulated as trait substitution sequences based on the fitness function given by Eq. (13), following Ito and Sasaki (2020, 2023). Red and blue dots indicate the dimorphic residents at the end of simulation. Red dashed lines in the left-most panels indicate the direction $\mathbf{e} = (1,0)^{\mathrm{T}}$ of dimorphic divergence, given by Eq. (15).

The right-most panel shows the time changes of the value for the function $H = H_C + H_D$ defined in Eq. (17). Under the existence of an inevitable branching point, as shown in panel (c), H works as a local Lyapunov function ensuring the steady progress of evolutionary branching. Parameters: $\sigma = 0.005$ and $\mathbf{D} = \begin{pmatrix} D_{xx} & D_{xy} \\ D_{xy} & D_{yy} \end{pmatrix} = \begin{pmatrix} 2 & 0 \\ 0 & -2 \end{pmatrix}$ for all (a-c); $\mathbf{C} = \begin{pmatrix} C_{xx} & C_{xy} \\ C_{yx} & C_{yy} \end{pmatrix} = \begin{pmatrix} 0.5 & 3 \\ -3 & -2 \end{pmatrix}$ for (a), $\mathbf{C} = \begin{pmatrix} -0.5 & 3 \\ -3 & -2 \end{pmatrix}$ for (b), and $\mathbf{C} = \begin{pmatrix} -0.5 & 0 \\ 0 & -2 \end{pmatrix}$ for (c).

Figure 2

Evolutionary branching in individual-based stochastic simulation under assumption of non-rare mutation (and asexual reproduction), for the same ecological settings with panels (a-c) in Fig. 1. The dynamics of phenotype distribution in trait space $\mathbf{s} = (x, y)^{\mathrm{T}}$ were projected onto the x-y plane (left), x-t plane (center), and y-t plane (right), where colored areas indicate observation of at least one individual. The color gradation indicates time, i.e., green and blue colors respectively indicate the initial and last states of the simulation. The black contours in the center and left panels indicate 20 and 200 individuals. The evolutionary dynamics was simulated by the same algorithm for sexual populations in Ito and Dieckmann (2007) except that all individuals reproduce clonally here. Individuals are diploid and each trait's value is the mean of additive loci containing integers. Parameters for ecological settings are the same with those used in Fig.1. Parameters for reproduction and mutation are as follows. Birth rate for phenotype $\mathbf{s}$: $b(\mathbf{s}) = 1$, death rate: $d(\mathbf{s}) = 1 - F(\mathbf{s}; (\mathbf{s}_1, \dots, \mathbf{s}_M), (n_1, \dots, n_M)/K_0)$ with $K_0 = 5000$, number of loci (diploid): 30, mutation rate per locus (stepwise mutation): 5×10^{-4}. K_0 roughly gives the number of individuals sustained in the system.

Figure 3

Collapse of dimorphic divergence observed in a three-dimensional trait space $\mathbf{s} = (x, y, w)^{\mathrm{T}}$ when the first three in the branching possibility conditions (Eq. (14)) are satisfied but the last one is not. Plotting formats are the same as those shown in the panels (except the right-most) of Fig. 1.

Figure 4

Effect of imaginary parts for eigenvalues of $\mathbf{C}$ on likelihood of evolutionary branching induced by a strongly possible branching point in two-dimensional trait space. $\mathbf{C}$, $\mathbf{D}$, and $\mathbf{V}_\mu$ are given by Eq. (19) with 100 different values for a chosen from 0.01 to 10 in a geometric manner, whereas σ was fixed at $\sigma = 0.005$. The initial monomorphic resident was fixed at $\mathbf{s}_0 = (100\sigma, 0)^{\mathrm{T}}$. The evolutionary dynamics was calculated with the same manner as those shown in Fig. 1. Each simulation has ended when evolutionary branching has occurred or when the path length (σK with K describing the numbers of invasions) has exceeded $10\, l_{\mathrm{CE}}(\mathbf{s}_0, \Delta s)$, where $l_{\mathrm{CE}}(\mathbf{s}_0, \Delta s)$ describes the path length expected with the canonical equation from the initial monomorphic resident $\mathbf{s}_0$ to the emergence of dimorphism with $\Delta s = 100\sigma$, defined in Eq. (S.2.70) in Appendix S2.6.

In panel (a), blue small "∘"s and "×"s indicate occurrence and non-occurrence of evolutionary branching with a for the horizontal axis and the path length for vetrical axis, where red and black curves indicate $10 l_{\mathrm{CE}}(\mathbf{s}_0, \Delta s)$ and $l_{\mathrm{CE}}(\mathbf{s}_0, \Delta s)$, respectively. In panel (b), blue small "∘"s and "×"s indicate occurrence and non-occurrence of evolutionary branching with a for the horizontal axis and the normalized path lengths ($\sigma K \,/\, l_{\mathrm{CE}}(\mathbf{s}_0, \Delta s)$) for the vertical axis. The black staircase plot and the green small "+"s indicate the mean path length (with errorbars indicating standard deviations) and the branching frequency, respectively, for subdivided regions of the horizontal axis. Panel (c) is plotted in the same manner as panel (b) except that the horizontal axis is $\log Q$ with Q defined in Eq. (20). The black vertical dashed line in panel (c) indicates $\log Q = 0$ (i.e., $Q = 1$). Panel (d) shows an example of evolutionary dynamics under $a = 0.01$ with the same plotting formats as those shown in Fig. 3, except that yellow triangles indicate the initial phenotype $\mathbf{s}_0 = (0.05, 0)^{\mathrm{T}}$, and that red circle shows the expected magnitude of the orbit radius (Eq. (S5.13) in Appendix S5).

Figure 5

Examination of heuristically developed index Q (Eq. (20)) for predicting likelihood of evolutionary branching in simulated evolution (for two-, three-, four-, and six-dimensional trait spaces, i.e., $L = 2,3,4,6$). Plotting formats for each panel is the same as those shown in panels (b) and (c) of Fig. 4, except that magenta color indicates possible branching points that are not strongly possible branching points. The simulation was repeated 500 times, where each simulation was conducted in the same manner with the simulation shown in Fig. 4, except that the initial phenotype $\mathbf{s}_0$ and the set of $\mathbf{C}$ and $\mathbf{D}$ (satisfying branching possibility conditions) were randomly chosen as described in the caption of Fig. S2 in Appendix S5.

Figure 6

Parameter dependency of three classes of evolutionary branching points in the model for the application example in Section 4. Parameters: $\sigma_\alpha = \sigma_\beta = 0.5$, and $\rho = 0.5$ for all panels (a-c); $c = 1, 0.5$, and 0 for panels (a), (b), and (c), respectively; $(r_{xx}, r_{yy}) = (1.5, -3.5)$, $(-0.5, -3.5)$, and $(-1, -1)$ for "**A**", "**B**", and "**C**", respectively.

Figure 7

Numerically simulated evolutionary branching induced by a possible, strongly possible, or inevitable branching point in the model for an application example in Section 4. Evolutionary dynamics was simulated in the same manner as those shown in Fig. 1, except that the fitness function was given by Eq. (21). Parameter values for (a), (b) and (c) are the same with those for "**A**", "**B**", and "**C**" in Fig. 5.

Figure 8

Evolutionary branching in individual-based stochastic simulation under assumption of non-rare mutation (and asexual reproduction), for the same ecological settings with panels (a-c) in Fig. 7. Plotting formats are the same as in Fig. 2, except that the black contours in the center and left panels indicate 10 and 100 individuals. The evolutionary dynamics was simulated in the manner same with the evolutionary dynamics shown in Fig. 2. Parameters for reproduction and mutation: $b(\mathbf{s}) = 1$, $d(\mathbf{s}) = 1 - F(\mathbf{s}; (\mathbf{s}_1, \dots, \mathbf{s}_M), (n_1, \dots, n_M)/K_0)$ with $K_0 = 2000$, number of loci (diploid): 30, mutation rate per locus (stepwise mutation): 5×10^{-4}.

(a) Possible branching point

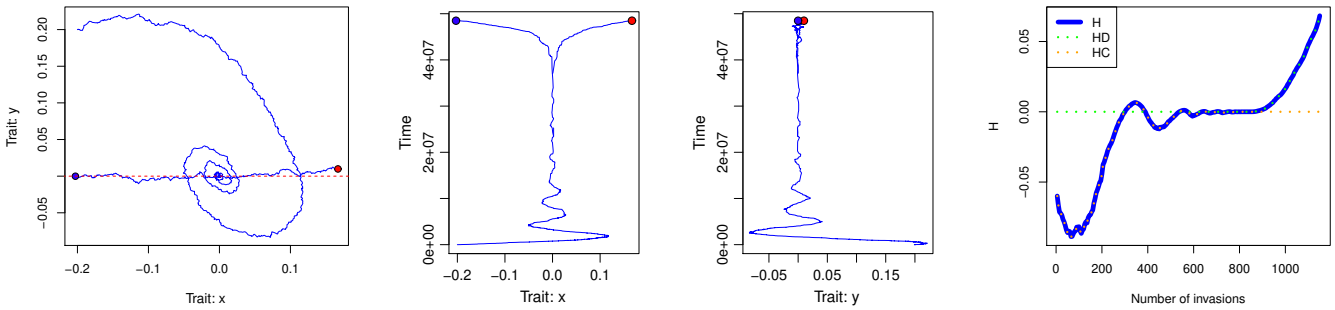

(b) Strongly possible branching point

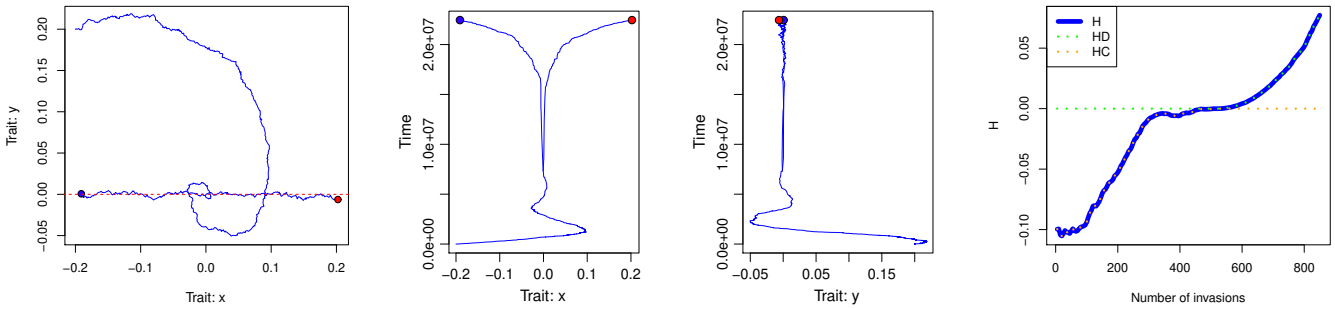

(c) Inevitable branching point

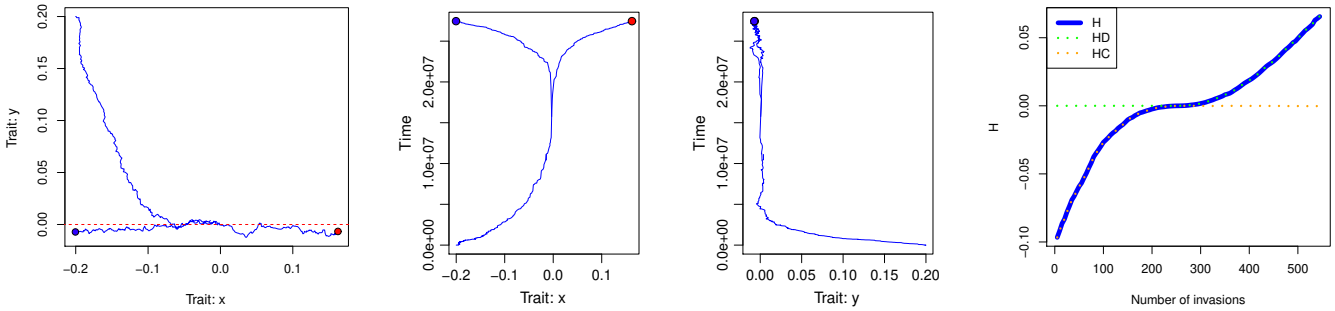

Figure 1.

Figure 2 Ito & Sasaki

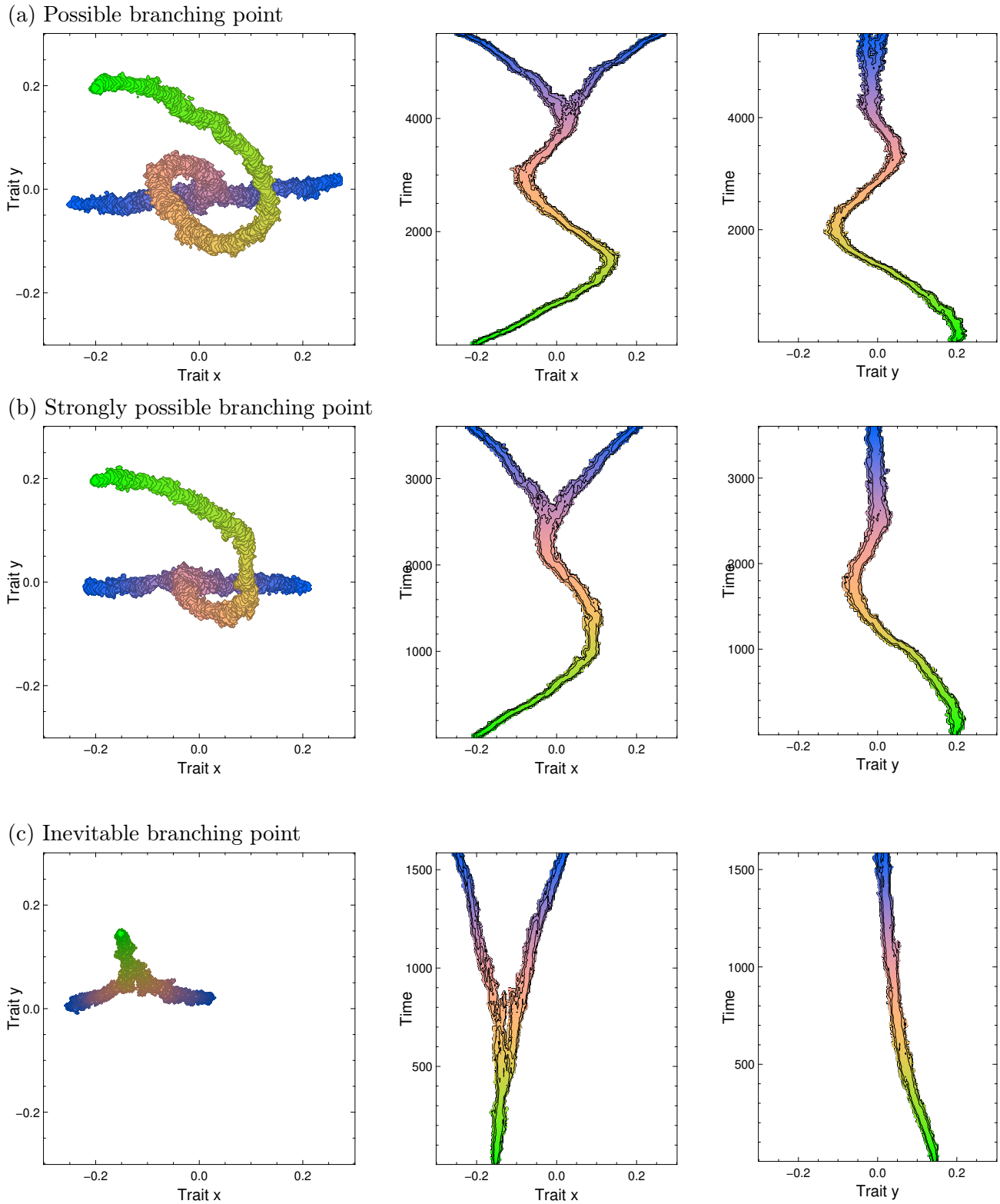

Figure 2.

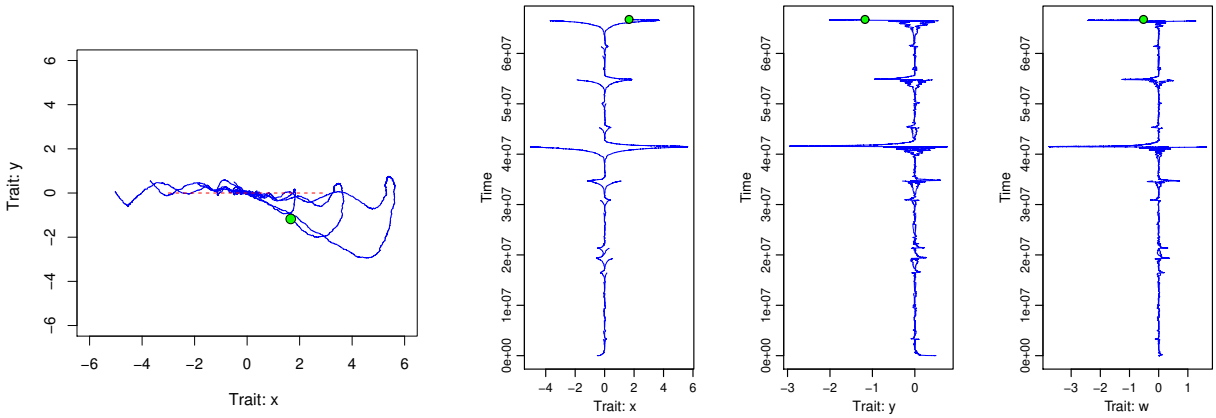

Figure 3.

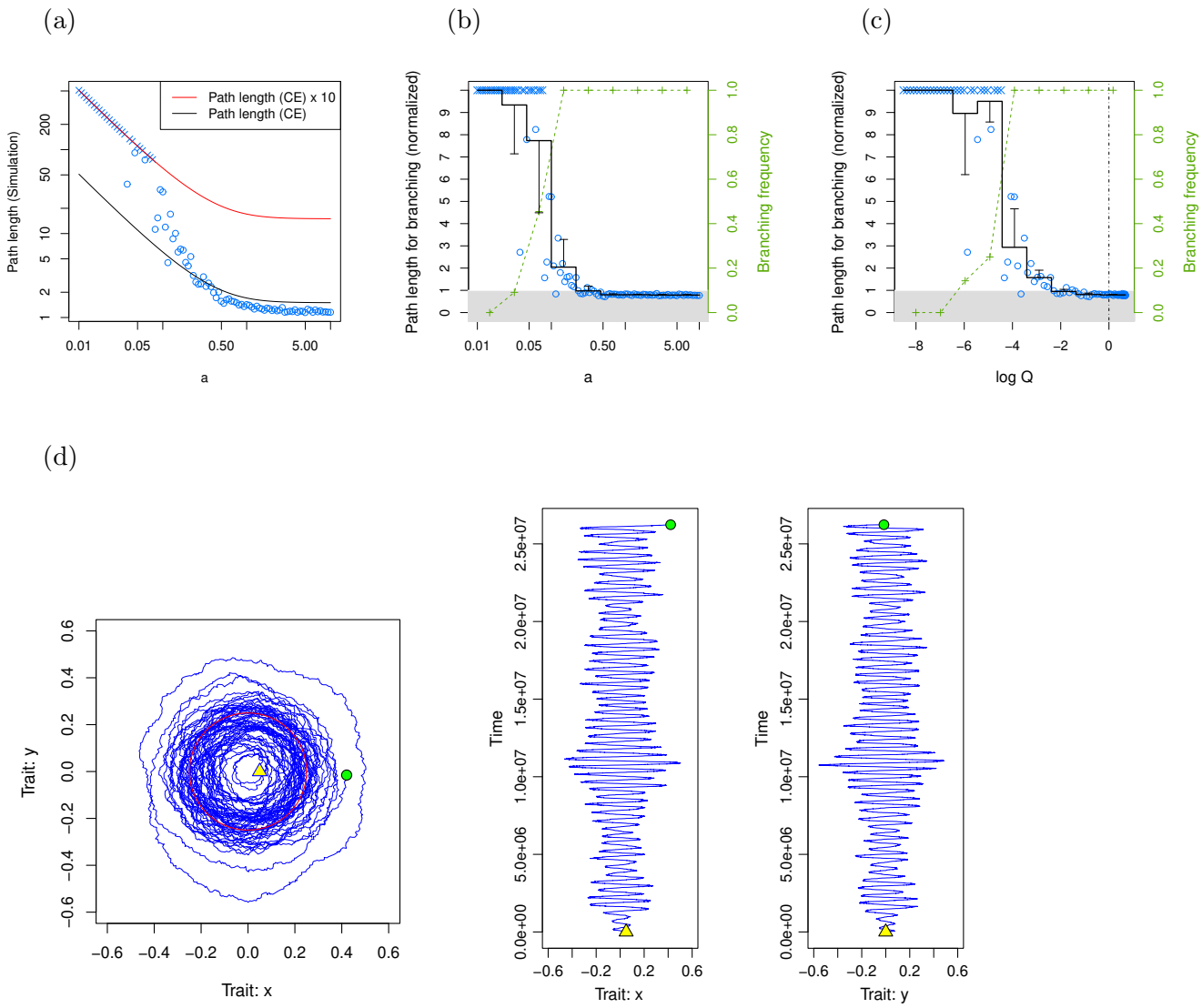
(a)
(b)
(c)
Path length (CE) x 10
Path length (CE)
Path length (Simulation)
a
Path length for branching (normalized)
Branching frequency
log Q
(d)
Trait: y
Trait: x
Time

Figure 4.

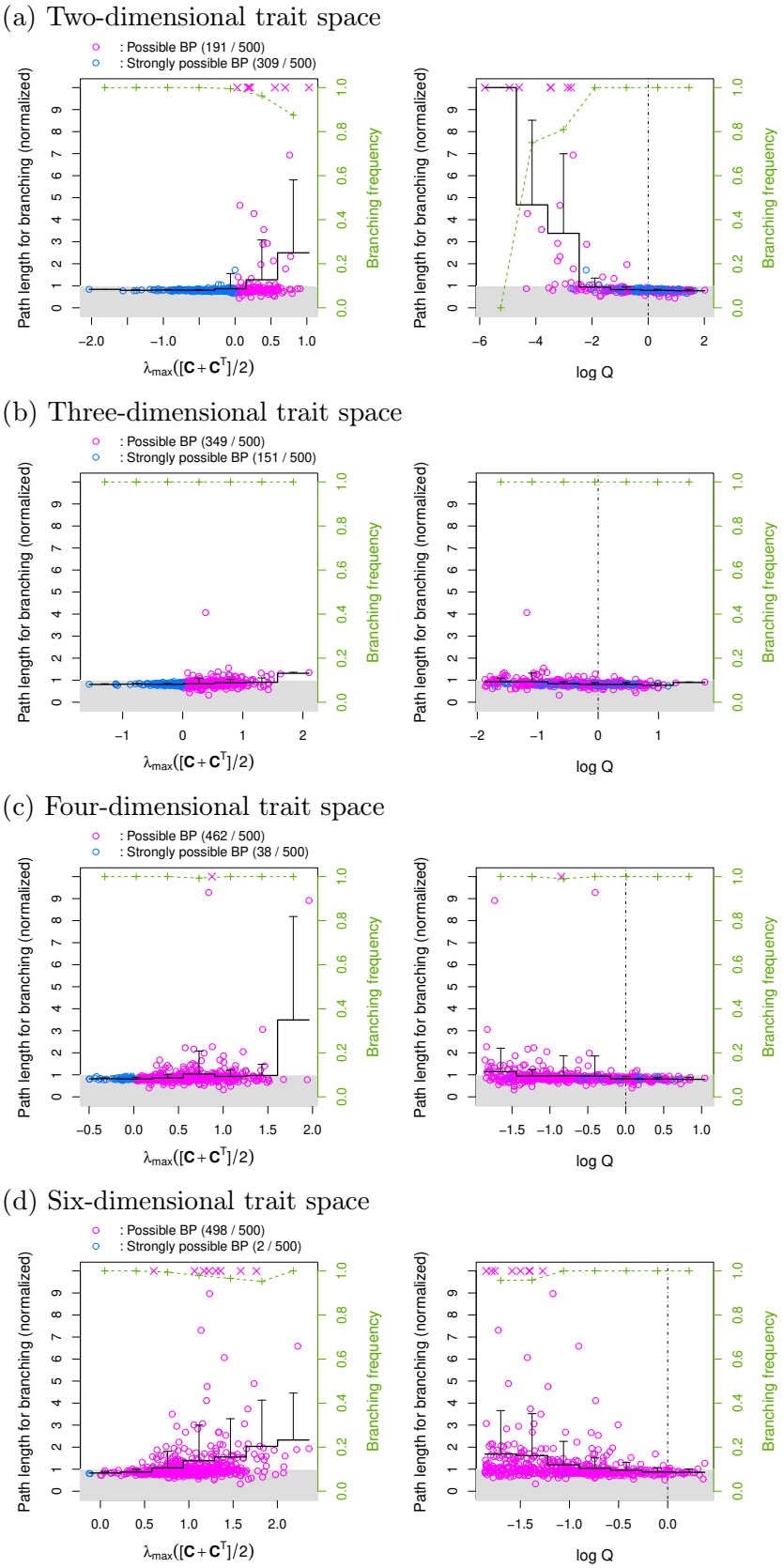
(a) Two-dimensional trait space
: Possible BP (191 / 500)
: Strongly possible BP (309 / 500)
(b) Three-dimensional trait space
: Possible BP (349 / 500)
: Strongly possible BP (151 / 500)
(c) Four-dimensional trait space
: Possible BP (462 / 500)
: Strongly possible BP (38 / 500)
(d) Six-dimensional trait space
: Possible BP (498 / 500)
: Strongly possible BP (2 / 500)
Path length for branching (normalized)
Branching frequency
λmax([C+C^T]/2)
log Q

Figure 5.

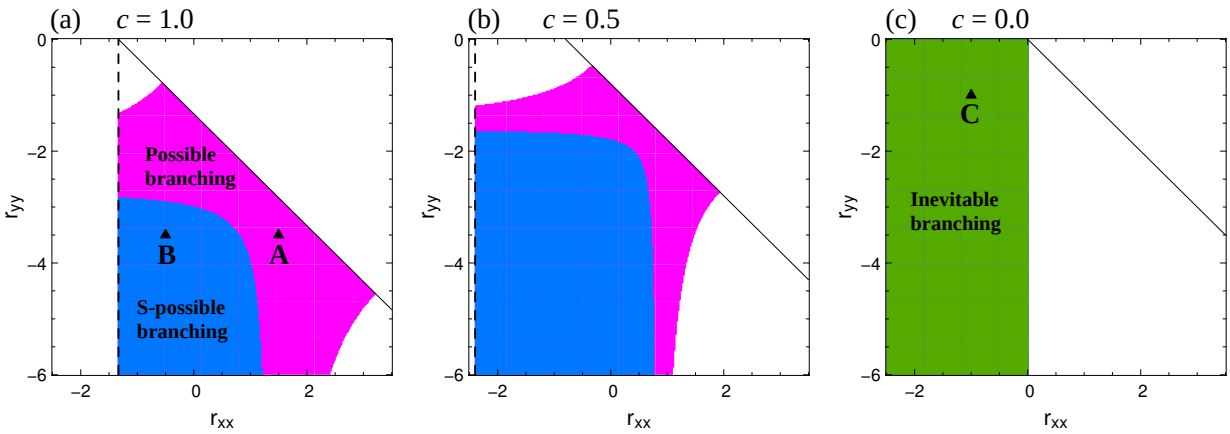
(a) c = 1.0
(b) c = 0.5
(c) c = 0.0
Possible branching
S-possible branching
Inevitable branching
A
B
C
r_yy
r_xx
0
−2
−4
−6
−2
0
2

Figure 6.

(a) Possible branching point ("A" in Fig. 5)

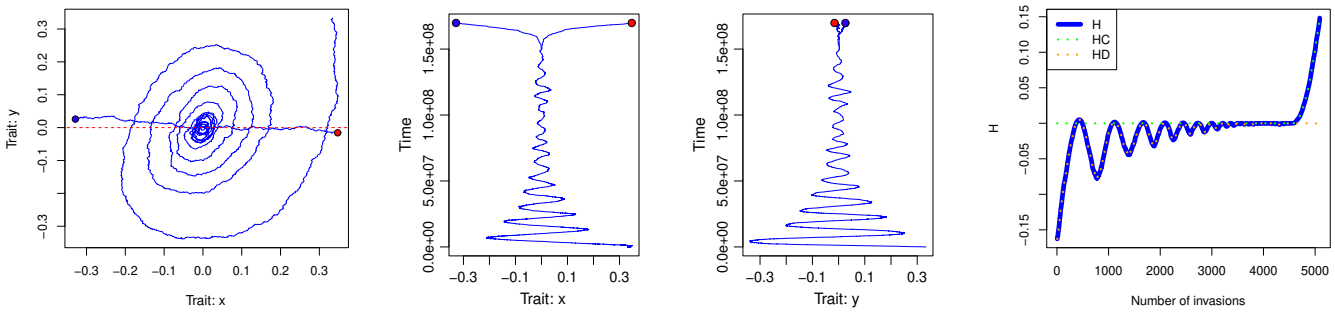

(b) Strongly possible branching point ("B" in Fig. 5)

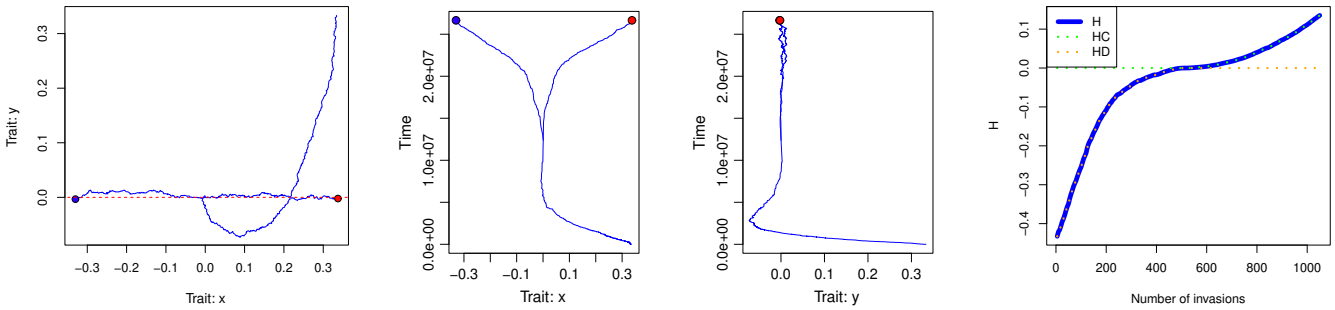

(c) Inevitable branching point ("C" in Fig. 5)

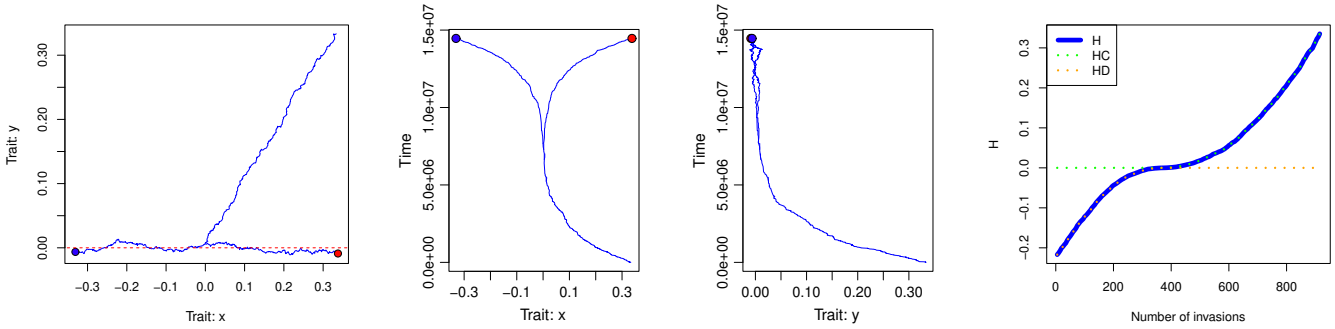

Figure 7.

(a) Possible branching point

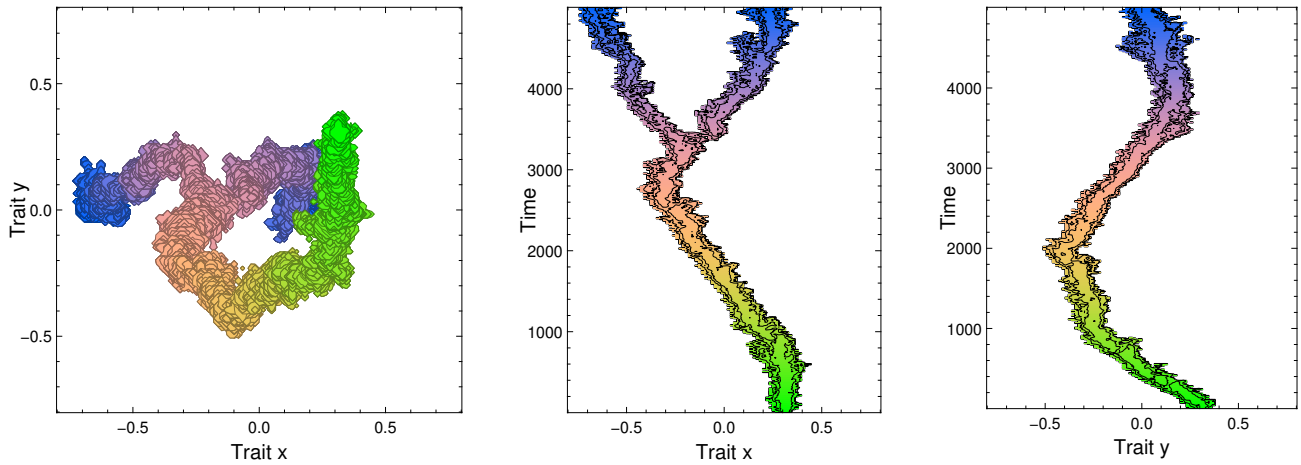

(b) Strongly possible branching point

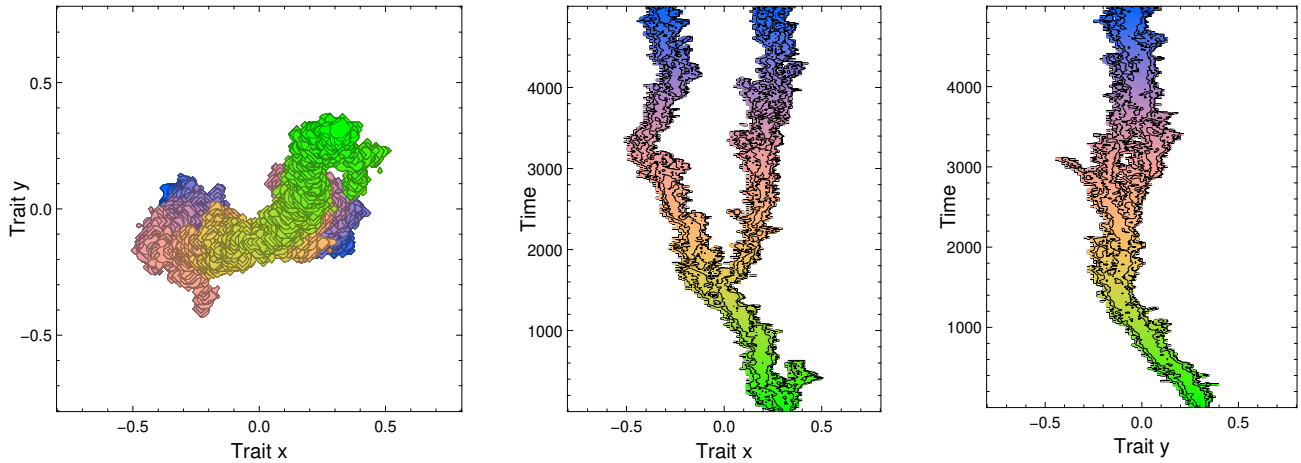

(c) Inevitable branching point

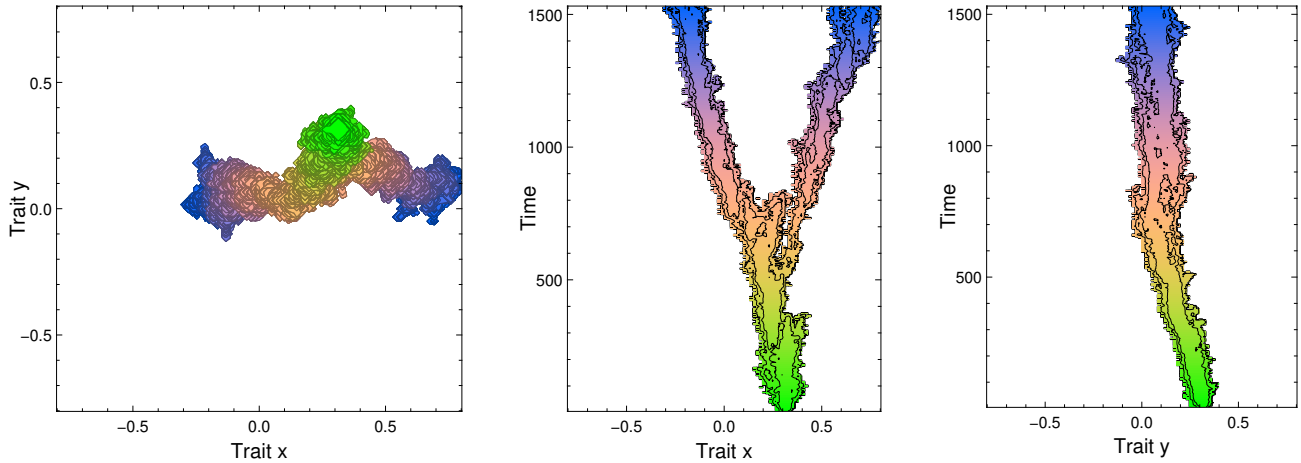

Figure 8.